Discrete Applied Mathematics 354 (2024) 29–47

Contents lists available at ScienceDirect

Discrete Applied Mathematics

journal homepage: www.elsevier.com/locate/dam

Embedding $K_{3,3}$ and K_5 on the double torus

Andrei Gagarin [a,*], William L. Kocay [b]

[a] School of Mathematics, Cardiff University, Cardiff, CF24 4AG, UK
[b] University of Manitoba, Computer Science Department, Winnipeg, Manitoba, R3T 2N2, Canada

ARTICLE INFO

Article history:
Received 31 October 2020
Received in revised form 5 April 2022
Accepted 20 May 2023
Available online 1 July 2023

Keywords:
Polygonal representations of orientable topological surfaces
Non-planar graphs
2-cell embeddings on the double and triple tori
Rotation system
Isomorphism
Tilings of the hyperbolic plane

ABSTRACT

The Kuratowski graphs $K_{3,3}$ and K_5 characterize planarity. Counting distinct 2-cell embeddings of these two graphs on orientable surfaces was previously done by Mull (1999) and Mull et al. (2008), using Burnside's Lemma and automorphism groups of $K_{3,3}$ and K_5, without actually constructing the embeddings. We obtain all 2-cell embeddings of these graphs on the double torus, using a constructive approach. This shows that there is a unique non-orientable 2-cell embedding of $K_{3,3}$, and 14 orientable and 17 non-orientable 2-cell embeddings of K_5 on the double torus, which are explicitly obtained using an algorithmic procedure of expanding from minors. Therefore we confirm the numbers of embeddings obtained by Mull (1999) and Mull et al. (2008). As a consequence, several new polygonal representations of the double torus are presented. Rotation systems for the one-face embeddings of K_5 on the triple torus are also found, using exhaustive search.

1. Introduction

The Kuratowski graphs $K_{3,3}$ and K_5 are well-known fundamental non-planar graphs, e.g., see [9]. The distinct (non-isomorphic) embeddings of $K_{3,3}$ and K_5 on the torus are known and can be found, e.g., in [3,8]. We want to find explicitly all distinct 2-cell embeddings of these two graphs on the double torus, which can serve as a first step in the study of graphs embeddable on the double torus. The number of 2-cell embeddings of these graphs on orientable surfaces was previously determined by Mull, Rieper, and White [12], and Mull [11], using Burnside's Lemma and automorphism groups of the graphs. In this paper, we use a constructive approach to find the embeddings and to determine their orientability. By Euler's formula for the double torus, we have $n+f-\varepsilon=-2$, implying that a 2-cell embedding of $K_{3,3}$ has $f=1$ face and a 2-cell embedding of K_5 has $f=3$ faces.

Graphs we consider in this paper can contain parallel edges (i.e., be multi-graphs), but not loops. A 2-cell embedding of a graph G on an oriented surface is characterized by its *rotation system*. Given a labelling of the vertices and edges, a rotation system consists of a cyclic list of the incident edges for each vertex v, called the *rotation* of v. The rotation system uniquely determines the facial boundaries, and therefore the embedding of G on the surface. If τ is a rotation system for an embedding of G, we denote the embedding by G^{τ}. Two embeddings G^{τ_1} and G^{τ_2} are isomorphic if there is a permutation of the vertices $V(G)$ and of the edges $E(G)$ that transforms τ_1 into τ_2. See [8] for more information on graph embeddings and rotation systems.

A graph is a *minor* of another graph if it can be obtained from the latter graph by deleting some of its edges and/or vertices and by contracting some of its edges. We denote by Θ_m a multi-graph consisting of two vertices $\{u, v\}$ and a set

* Corresponding author.
E-mail address: gagarina@cardiff.ac.uk (A. Gagarin).

https://doi.org/10.1016/j.dam.2023.05.018

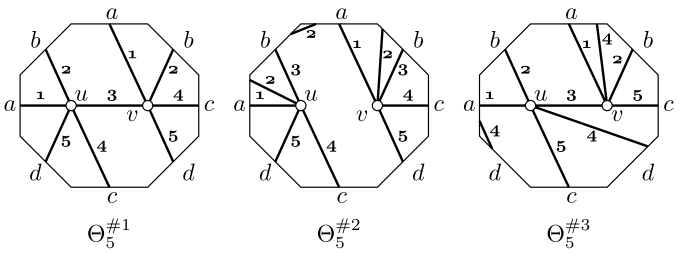

Fig. 1. Three distinct 2-cell embeddings of Θ_5 on the double torus. The edges are numbered.

of m parallel edges between them ($m \geq 1$). This graph can be considered as a generalized theta graph. In what follows, we first construct all 2-cell embeddings of an auxiliary graph Θ_5 on the double torus, and then derive all possible embeddings of $K_{3,3}$ and K_5 on this surface by expanding Θ_5 and some other minors of $K_{3,3}$ and K_5 back to the original graphs. This is done in Sections 2, 3, and 5. Section 4 provides different polygonal representations of the double torus, based on the results of Sections 2 and 3. Section 6 and Appendices conclude the paper, explicitly describing all rotation systems for 2-cell embeddings of K_5 on the double and triple tori, and providing corrections to some numerical results from [3] for embeddings on the torus.

2. Θ_5 on the double torus

The multi-graph Θ_5 satisfies Euler's formula, with $f = 1$ for the double torus. Three 2-cell embeddings of Θ_5 on the double torus are shown in Fig. 1. Here the double torus is represented by a standard octagon $a^+b^+a^-b^-c^+d^+c^-d^-$, traversed clockwise, with paired sides $\{a, b, c, d\}$. See [2,5,6,13,14,16] for more information on representations of the double torus.

We first need to show that these comprise all distinct 2-cell embeddings of Θ_5. They all have a single face, homeomorphic to an open disc, with facial boundary C consisting of 10 edges. The octagon representation $a^+b^+a^-b^-c^+d^+c^-d^-$ of the double torus determines a *tiling of the hyperbolic plane by regular octagons*, which is invariant under a group of translation symmetries, see [8,14]. The translations are those that map the fundamental octagon to other octagons in the tiling, such that side a is mapped to another side a, side b to another side b, and so forth. The group of translations is transitive on the octagons. When the double torus is cut (see [2,5]) to produce the standard octagon $a^+b^+a^-b^-c^+d^+c^-d^-$, the octagon becomes the fundamental region of the group of translation symmetries, and its boundary cycle C corresponds to a Jordan curve in the hyperbolic plane.

In general, a Jordan curve bounding a fundamental region in the hyperbolic plane, which we will also denote by C, has an interior that is equivalent to the interior of the fundamental octagon, in the sense that every point in the octagon, except points of its boundary cycle, is equivalent to exactly one point in the interior of the Jordan curve C under the action of the translation symmetries. In other words, the interior of C can also be taken as a fundamental region for the group of translations of the hyperbolic plane. Every 2-cell embedding of Θ_5 on the double torus has an associated Jordan curve with this property.

Theorem 1. *There are exactly three distinct 2-cell embeddings of Θ_5 on the double torus.*

Proof. There are eight octagons that meet at each of the octagon corner vertices in the hyperbolic plane (e.g., see Fig. 2). Let the vertices of Θ_5 be $\{u, v\}$. By Euler's formula, there must be just one face in a 2-cell embedding of Θ_5 on the double torus. Without loss of generality, place u near that corner of the octagon where side a meets side d, and place v near the corner of the octagon where side b meets side c. In the tiling of the hyperbolic plane generated by translations of the fundamental octagon, a copy of u and v will appear in each octagon. At every corner vertex of the octagon, the sides appear in the cyclic clockwise order as $(b^+, a^-, b^-, a^+, d^+, c^-, d^-, c^+)$. This is illustrated in Fig. 2, where the eight octagons surrounding a corner vertex are illustrated schematically. Here copies of vertex u are shaded light grey, and copies of v are shaded dark grey.

Denote by C the Jordan curve in the hyperbolic plane corresponding to the unique facial cycle of Θ_5 when embedded on the double torus with a 2-cell face. The five edges of Θ_5 each appear twice on the boundary of C, which is a 10-gon, so that the vertices of the cycle alternate $(v, u, v, u, v, u, v, u, v, u)$, and each edge is traversed exactly once in each direction. The translation symmetries of the hyperbolic plane will map C to copies of C, such that their interiors are disjoint and, together with C and its translations, cover the entire hyperbolic plane.

Without loss of generality, the interior of C can be taken to contain the central corner vertex of the diagram in Fig. 2. However, it must not contain any other corner vertices, as those are obtained by translations of the central corner vertex. Therefore C is a Jordan curve in the hyperbolic plane whose interior contains the central corner vertex in Fig. 2. An example of a similar situation occurs when graphs are embedded on the torus. Fig. 3 shows two (equivalent) embeddings

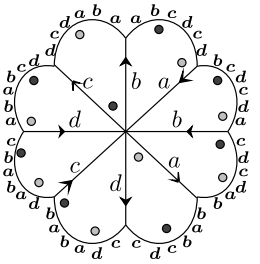

Fig. 2. The eight octagons meeting at one corner vertex.

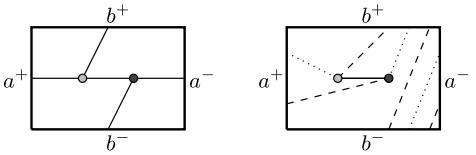

Fig. 3. Two equivalent embeddings of Θ_3 on the torus.

of Θ_3 on the torus. The embedding on the right is somewhat "skewed", crossing the rectangle boundary several times, but it is nevertheless an equivalent embedding with a single face (see also Figure 2 in [3] and corresponding explanation at the beginning of Section 2 in [3]).

As a result, the 10 edges of C must intersect all of the eight octagon sides incident on the central corner vertex. So, we can write $C = (v, s_1, u, s_2, v, \ldots, u, s_{10})$, where each s_i is a label corresponding to a traversal of an edge of the facial cycle of Θ_5 – it represents a string of zero or more letters, corresponding to the sides of the octagons crossed by the corresponding edge of C, $i = 1, \ldots, 10$. For example, if edge i crosses an octagon side labelled a, then s_i will be one of a^+ or a^-, depending on the direction in which side a is crossed. When travelling along C, there is a region to the right and a region to the left. When an edge of C crosses a side of the octagon directed from the right to the left of C, this will be denoted by $+$. So $s_i = a^+$ means that edge i of C crosses the octagon side labelled a, directed from the right to the left. If the edge of C crosses two or more sides of the octagon, then s_i will be a string of two or more letters, e.g., $s_i = b^+a^-$, or $s_i = b^+a^-c^+$, etc. Note that an edge uv of C can cross any sequence of octagon sides, as long as C does not enclose any corners other than the central corner. If the edge does not cross any edges of the octagon, then we write $s_i = \phi$.

As each edge of Θ_5 occurs twice on C, with opposite orientations, there is an s_j corresponding to each s_i such that $s_j = s_i^{-1}$, where $j \neq i$. For example, if $s_i = b^+a^-c^+$, then $s_j = s_i^{-1} = c^-a^+b^-$. Concatenating all the strings s_i on the cycle C, $i = 1, \ldots, 10$, gives the string $(s_1 s_2 \ldots s_{10})$, which must reduce to a cyclic permutation of $(b^+a^-b^-a^+d^+c^-d^-c^+)$, namely the cyclic sequence of octagon sides incident on the central corner vertex in Fig. 2. Note that there will be at most one $s_i = \phi$ (and its inverse), for otherwise the embedding would have a digon face, which is not the case here.

Therefore, we have a cycle of ten edge labels $(s_1, s_2, \ldots, s_{10})$, consisting of five strings and their inverses. Let the five strings be denoted by $\alpha, \beta, \rho, \sigma, \mu$ and their inverses by $\alpha^{-1}, \beta^{-1}, \rho^{-1}, \sigma^{-1}, \mu^{-1}$. If $s_i = \alpha$, then α^{-1} can only be some s_j such that $j \not\equiv i \pmod 2$, i.e., i and j must have opposite parity. This is because each edge of Θ_5 is traversed exactly twice on C, in *opposite* directions, and the vertices of C alternate $u, v, u, v, \ldots$. Furthermore, for each string, for example α, if $s_i = \alpha$, we have $\alpha^{-1} \neq s_{i\pm1}$, or else $\alpha\alpha^{-1}$ or $\alpha^{-1}\alpha$ would cancel, which is not possible. Here arithmetic on the subscripts is done mod 10, such that the result is a number in the range $1 \ldots 10$.

We first show that there are at most five ways to assign the labels of strings to the cycle edges. Without loss of generality, let $s_1 = \alpha$. Then α^{-1} is either s_4 or s_6. Note that we need not consider s_8 as α^{-1}, as this is equivalent to reversing the cycle. This gives two cases:

(1) $(\alpha, s_2, s_3, \alpha^{-1}, s_5, s_6, s_7, s_8, s_9, s_{10})$

(2) $(\alpha, s_2, s_3, s_4, s_5, \alpha^{-1}, s_7, s_8, s_9, s_{10})$

We can characterize these cases by saying that in Case (1) at least one of the pairs $(\alpha, \alpha^{-1}), (\beta, \beta^{-1}), (\sigma, \sigma^{-1}), (\rho, \rho^{-1})$, or (μ, μ^{-1}) occurs as s_i and $s_{i\pm3}$, and in Case (2) no pair $(\alpha, \alpha^{-1}), (\beta, \beta^{-1}), (\sigma, \sigma^{-1}), (\rho, \rho^{-1})$, or (μ, μ^{-1}) occurs as s_i and $s_{i\pm3}$, i.e. every pair $(\alpha, \alpha^{-1}), (\beta, \beta^{-1}), (\sigma, \sigma^{-1}), (\rho, \rho^{-1})$, and (μ, μ^{-1}) occurs as s_i and $s_{i\pm5}$. This division into two cases results in a number of subsequent cases. First of all, we have a unique completion for Case (2):

$$(\alpha, \beta, \sigma, \rho, \mu, \alpha^{-1}, \beta^{-1}, \sigma^{-1}, \rho^{-1}, \mu^{-1}) \qquad (*)$$

In Case (1), without loss of generality, we can choose s_6 as β. Then β^{-1} is either s_3 or s_9, giving two sub-cases:

(1a) $(\alpha, s_2, \beta^{-1}, \alpha^{-1}, s_5, \beta, s_7, s_8, s_9, s_{10})$

(1b) $(\alpha, s_2, s_3, \alpha^{-1}, s_5, \beta, s_7, s_8, \beta^{-1}, s_{10})$

In Case (1a), without loss of generality, we can choose s_8 as σ. Then σ^{-1} is s_5, giving

(1ai) $(\alpha, s_2, \beta^{-1}, \alpha^{-1}, \sigma^{-1}, \beta, s_7, \sigma, s_9, s_{10})$

We then can choose s_9 as ρ, which requires ρ^{-1} to be s_2. Then s_7 is μ and s_{10} is μ^{-1}:

$$(\alpha, \rho^{-1}, \beta^{-1}, \alpha^{-1}, \sigma^{-1}, \beta, \mu, \sigma, \rho, \mu^{-1}) \qquad (*)$$

In Case (1b), we can choose s_7 as σ. Then σ^{-1} is either s_2 or s_{10}:

(1bi) $(\alpha, \sigma^{-1}, s_3, \alpha^{-1}, s_5, \beta, \sigma, s_8, \beta^{-1}, s_{10})$

(1bii) $(\alpha, s_2, s_3, \alpha^{-1}, s_5, \beta, \sigma, s_8, \beta^{-1}, \sigma^{-1})$

In Case (1bi), we can choose s_3 as ρ. Then ρ^{-1} is either s_8 or s_{10}. Each results in a unique completion:

$$(\alpha, \sigma^{-1}, \rho, \alpha^{-1}, \mu, \beta, \sigma, \rho^{-1}, \beta^{-1}, \mu^{-1}) \qquad (*)$$

$$(\alpha, \sigma^{-1}, \rho, \alpha^{-1}, \mu, \beta, \sigma, \mu^{-1}, \beta^{-1}, \rho^{-1}) \qquad (*)$$

In Case (1bii), we can choose s_2 as ρ. Then ρ^{-1} is s_5. There is a unique completion:

$$(\alpha, \rho, \mu, \alpha^{-1}, \rho^{-1}, \beta, \sigma, \mu^{-1}, \beta^{-1}, \sigma^{-1}) \qquad (*)$$

This gives five possible solutions for labelling the facial cycle edges. We rename the letters so that each solution begins with $(\alpha, \beta, \rho, \alpha^{-1}, \ldots)$, except for the first one found. The results are:

$$A = (\alpha, \beta, \rho, \sigma, \mu, \alpha^{-1}, \beta^{-1}, \rho^{-1}, \sigma^{-1}, \mu^{-1})$$
$$B = (\alpha, \beta, \rho, \alpha^{-1}, \sigma, \rho^{-1}, \mu, \sigma^{-1}, \beta^{-1}, \mu^{-1})$$
$$F = (\alpha, \beta, \rho, \alpha^{-1}, \sigma, \mu, \beta^{-1}, \rho^{-1}, \mu^{-1}, \sigma^{-1})$$
$$D = (\alpha, \beta, \rho, \alpha^{-1}, \sigma, \mu, \beta^{-1}, \sigma^{-1}, \mu^{-1}, \rho^{-1})$$
$$E = (\alpha, \beta, \rho, \alpha^{-1}, \beta^{-1}, \sigma, \mu, \rho^{-1}, \sigma^{-1}, \mu^{-1})$$

We first show that cyclic sequences A, B, and E can be realized by suitable choices of strings for labels. If we choose $\alpha = b^+, \beta = a^-, \rho = \phi, \sigma = d^+, \mu = c^-$, we obtain $E = (b^+, a^-, \phi, b^-, a^+, d^+, c^-, \phi, d^-, c^+)$, which reduces to $(b^+a^-b^-a^+d^+c^-d^-c^+)$, as required. This solution is identical to the embedding $\Theta_5^{\#1}$ in Fig. 1, starting with s_4.

If we choose $\alpha = b^-, \beta = b^+a^+, \rho = a^-, \sigma = d^-, \mu = c^+$, we obtain $A = (b^-, b^+a^+, a^-, d^-, c^+, b^+, a^-b^-, a^+, d^+, c^-)$, which also reduces to $(b^+a^-b^-a^+d^+c^-d^-c^+)$. This solution is identical to the embedding $\Theta_5^{\#2}$ in Fig. 1, starting with s_1.

If we choose $\alpha = b^+, \beta = a^-, \rho = \phi, \sigma = a^+d^+, \mu = c^-$, we obtain $B = (b^+, a^-, \phi, b^-, a^+d^+, \phi, c^-, d^-a^-, a^+, c^+)$, which also reduces to $(b^+a^-b^-a^+d^+c^-d^-c^+)$. This solution is identical to the embedding $\Theta_5^{\#3}$ in Fig. 1, starting with s_1.

Therefore these three choices of strings for labels give three embeddings of Θ_5, each with one face. These three embeddings are pairwise non-isomorphic. For any string s_i occurring in A, its inverse is s_{i+5}, which is not the case with B or E. And for any string s_i occurring in B, its inverse is either s_{i+3} or s_{i-3}, which is not the case with E.

Clearly, any embeddings of Θ_5 corresponding to solutions A, B or E are isomorphic to one of these three, because the facial cycle determines the rotation system uniquely. Therefore each of the solutions A, B and E defines an isomorphism class of embeddings. Also, notice that renaming the strings of D as $\alpha \to \beta \to \rho \to \alpha^{-1}$ converts D (starting at s_{10}) into E. Therefore labellings D and E are equivalent.

We show that the remaining solution F cannot be realized by an embedding. Consider the cyclic product of strings $(s_1 \ldots s_{10})$. This must reduce to $(b^+a^-b^-a^+d^+c^-d^-c^+)$. Notice that the latter string has a decomposition into a substring based on $\{a, b\}$ and another substring based on $\{c, d\}$, and that they are disjoint. The letter diametrically opposite any letter a or b is c or d, respectively, and conversely. Consider the three edges of F labelled s_4, s_5, s_6. Their inverses are the edges labelled s_1, s_{10}, s_9, respectively. Suppose $s_5 = qrs$, where q is the longest prefix that cancels with a suffix of s_4, and s is the longest suffix of s_5 that cancels with a prefix of s_6. So, $s_4 = pq^{-1}$ and $s_6 = s^{-1}t$ for suitable strings p, q, r, s, t. Then $s_4s_5s_6 = pq^{-1}qrss^{-1}t = prt \neq \phi$, because $s_4s_5s_6 = \phi$ would mean a shorter cycle contained in C, a contradiction. The diametrically opposite string is $s_9s_{10}s_1 = s_6^{-1}s_5^{-1}s_4^{-1} = t^{-1}ss^{-1}r^{-1}q^{-1}qp^{-1} = t^{-1}r^{-1}p^{-1} = (prt)^{-1}$, which contains the same letters as prt, a contradiction.

It follows that there are exactly three distinct 2-cell embeddings of Θ_5 on the double torus, shown in Fig. 1. □

2.1. Automorphisms, rotations, orientability

The automorphisms of the embeddings of Fig. 1 will be helpful in finding the embeddings of $K_{3,3}$. We will need the rotations at vertices u and v for each embedding, written explicitly below. The numbers below are the edge numbers in the embeddings of Fig. 1. An automorphism is a permutation of vertices and/or edges that leaves the rotation system unchanged. An embedding is *non-orientable* if the embedding obtained by reversing the rotations is isomorphic to the original embedding. Otherwise it is *orientable*.

$\Theta_5^{\#1}$	$u : (1, 2, 3, 4, 5)$	$v : (1, 2, 4, 5, 3)$
$\Theta_5^{\#2}$	$u : (1, 2, 3, 4, 5)$	$v : (1, 2, 3, 4, 5)$
$\Theta_5^{\#3}$	$u : (1, 2, 3, 4, 5)$	$v : (1, 4, 2, 5, 3)$

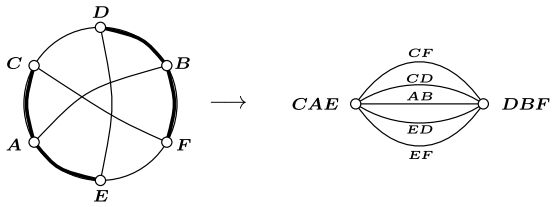

Fig. 4. $K_{3,3}$ and a minor isomorphic to Θ_5.

Lemma 2. *Embedding $\Theta_5^{\#1}$ of Fig. 1 has the automorphism group of order two and is non-orientable.*

Proof. The permutation $(u, v)(1, 4)(2, 5)$ interchanges the rotations of u and v, and so is an automorphism. It is the only possible non-trivial automorphism due to the unique position of edge 3 in the facial cycle: this is the only edge whose opposite traversal is diametrically opposite to itself on the cycle. See the unique face of $\Theta_5^{\#1}$ drawn in Fig. 13, where edge 3 of $\Theta_5^{\#1}$ in Fig. 1 is the side labelled e of the 10-gon. The permutation $(1, 5)(2, 4)$ maps the rotations of u and v to their reversals. Therefore, $\Theta_5^{\#1}$ is non-orientable. □

Lemma 3. *Embedding $\Theta_5^{\#2}$ of Fig. 1 has the automorphism group of order ten, is non-orientable, and all its edges are equivalent.*

Proof. It is clear from the rotations that permutations (u, v) and $(1, 2, 3, 4, 5)$ are automorphisms of $\Theta_5^{\#2}$. Therefore the group has order ten. The permutation $(2, 5)(3, 4)$ maps the rotations to their reversals, implying the embedding is non-orientable. □

Lemma 4. *Embedding $\Theta_5^{\#3}$ of Fig. 1 has the automorphism group of order five, is non-orientable, and all its edges are equivalent.*

Proof. From the rotations, we see that permutation $(1, 2, 3, 4, 5)$ is an automorphism of $\Theta_5^{\#3}$. This permutation generates the whole automorphism group. Therefore the group has order five. The permutation $(2, 5)(3, 4)$ maps the rotations to their reversals, implying the embedding is non-orientable. □

Corollary 5. *In each of the embeddings $\Theta_5^{\#1}$ and $\Theta_5^{\#2}$, vertices u and v are equivalent. They are not equivalent in $\Theta_5^{\#3}$.*

If uv is an edge of a graph G, we denote the graph obtained by contracting edge uv by $G \cdot uv$. Clearly, if uv belongs to a triangle in G, contracting uv will result in parallel edges in $G \cdot uv$, and contracting an edge xy from a set of parallel edges in G would create a loop in $G \cdot xy$. We will need the following simple lemma.

Lemma 6. *Suppose G^τ is a 2-cell embedding of a graph G (parallel edges are possible) on the double torus, no face of G^τ is a digon, and uv is a non-parallel edge of G which is not on a boundary of a triangular face of G^τ. Then $G^\tau \cdot uv$ is a 2-cell embedding of $G \cdot uv$ with no loops or digon facial cycles.*

Proof. Clearly, loops in $G^\tau \cdot uv$ and $G \cdot uv$ would only be possible if uv were from a set of parallel edges. So, $G^\tau \cdot uv$ and $G \cdot uv$ have no loops. Since uv is not on a boundary of a triangular face of G^τ, contracting uv does not create any digon faces in $G^\tau \cdot uv$. Clearly, contracting an edge on the boundary of a 2-cell face in G^τ leaves the corresponding face in the resulting embedding equivalent to an open disc (no loops in G here). □

3. $K_{3,3}$ on the double torus

Denote now by A, B, C, D, E, F the vertices of $K_{3,3}$, and choose the edges AC, AE, BD, BF (drawn in bold) of $K_{3,3}$ as shown in Fig. 4. Contract these four edges to form a minor of $K_{3,3}$ isomorphic to Θ_5. *If we start with a 2-cell embedding of $K_{3,3}$ on the double torus, after contracting the edges, the resulting embedding of the minor will be a 2-cell embedding of Θ_5 on the double torus.* This follows from Lemma 6 and the fact that no facial cycle of $K_{3,3}$ is a digon or triangle, as there is only one face in the embedding. Therefore, every 2-cell embedding of $K_{3,3}$ on the double torus can be contracted to a 2-cell embedding of Θ_5, and Θ_5 has only three 2-cell embeddings. To find the distinct 2-cell embeddings of $K_{3,3}$, we restore the contracted edges in all possible ways and compare the results for isomorphism.

The vertices of the resulting minor Θ_5 of $K_{3,3}$ will be denoted by CAE and DBF, corresponding to the vertices $\{A, C, E\}$ and $\{B, D, F\}$ of $K_{3,3}$ that were amalgamated during the edge-contractions. The edges of Θ_5 can be labelled AB, CD, CF, ED, EF, in correspondence to the edges of $K_{3,3}$ they are derived from (see Fig. 4). There are $5! = 120$ different ways to assign the labels AB, CD, CF, ED, EF to the five edges of the embeddings of Θ_5 shown in Fig. 1, before attempting to restore the contracted edges. However, many of them are equivalent.

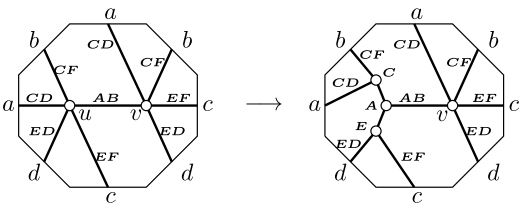

Fig. 5. Case of central edge labelled *AB*, impossible to extend.

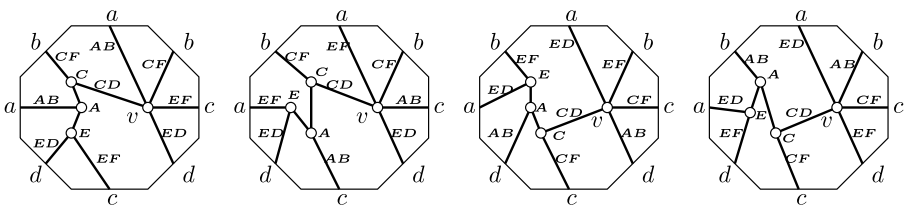

Fig. 6. Case of central edge *CD*.

Lemma 7. *There are eight automorphisms of $K_{3,3}$ that map the bold subgraph of Fig. 4 to itself, generated by the permutations* (CE), (DF), *and* $(AB)(CD)(EF)$.

It follows from Lemma 7 that, without loss of generality, vertex u of Θ_5 can be taken to be *CAE*, so that vertex v is *DBF*. Furthermore, the *central edge* uv in the embeddings #1 and #3 of Fig. 1, i.e., the only edge not crossing the boundary of the octagon, can be taken to be either *AB* or *CD*, as the non-contracted edges of $K_{3,3}$ in Fig. 4 are all equivalent to one of these.

So, we have an embedding of Θ_5 of Fig. 4, with the vertices labelled *CAE* and *DBF*, and the edges labelled *AB*, *CD*, *CF*, *ED*, *EF*. The embedding is one of $\Theta_5^{\#1}$, $\Theta_5^{\#2}$, $\Theta_5^{\#3}$ of Fig. 1. Vertex *CAE* is to be expanded into a path $[C, A, E]$, and *DBF* is to be expanded into a path $[D, B, F]$. When *CAE* is expanded, the five edges in the rotation of *CAE* must be divided into two consecutive edges for *C*, one edge for *A*, and two consecutive edges for *E*. A similar observation holds for *DBF*.

Lemma 8. *There are no extensions of $\Theta_5^{\#1}$ to $K_{3,3}$ with central edge uv labelled AB.*

Proof. Suppose that uv represents edge *AB*, as in Fig. 5. There are two ways to expand vertex u into the path $[C, A, E]$, having *AB* as the central edge. For each of these, the edges *CD* and *CF* must intersect consecutive sides of the octagon, and the edges *ED* and *EF* must also intersect consecutive sides of the octagon. One such arrangement is shown in Fig. 5. There are eight possible ways of arranging the labels of the edges incident on *C* and *D* with *CD*, *CF*, *ED*, *EF* satisfying this condition.

However, vertex v must be expanded into a path $[D, B, F]$, such that the edges *CD* and *ED* intersect consecutive sides of the octagon, and edges *EF* and *CF* intersect consecutive sides. By inspection of the eight arrangements, we see that this is not possible. □

Lemma 9. *There are four extensions of $\Theta_5^{\#1}$ to $K_{3,3}$ with central edge uv labelled CD.*

Proof. Suppose that central edge uv represents edge *CD*. There are eight ways of expanding vertex *CAE* into a path $[C, A, E]$, some of which are shown in Fig. 6. For each of these, edges *ED* and *EF* must be consecutive in the rotation of *E*, i.e. intersect consecutive sides of the octagon. However, edges *CF*, *EF* must also be consecutive in the rotation of *DBF*. This reduces the number of ways of expanding u to a path $[C, A, E]$ to four, which are shown in Fig. 6.

Vertex *DBF* must then be expanded into a path $[D, B, F]$. In each of the four cases, there is exactly one way to do this, as shown in Fig. 7. □

Lemma 10. *There are no extensions of $\Theta_5^{\#2}$ to $K_{3,3}$.*

Proof. We have vertex u of $\Theta_5^{\#2}$ representing the vertex *CAE*. The five incident edges correspond to *AB*, *CD*, *CF*, *DE*, *EF*. When *CAE* is expanded to the path $[C, A, E]$, the edges *CD*, *CF* must be consecutive, because they are both incident on *C*; and *EF*, *ED* must be consecutive, because they are both incident on *E*. The remaining edge must be *AB*. There are a number of ways of assigning names to the edges incident on vertex u satisfying this requirement. However, when vertex *DBF* (v

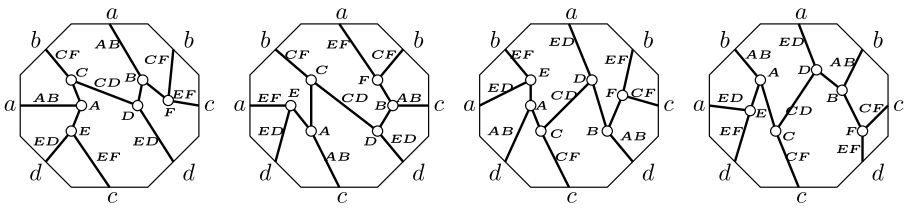

Fig. 7. Completion of the case of central edge *CD*.

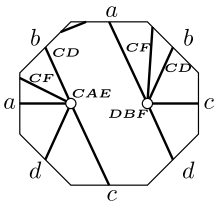

Fig. 8. There are no extensions of $\Theta_5^{\#2}$ to $K_{3,3}$.

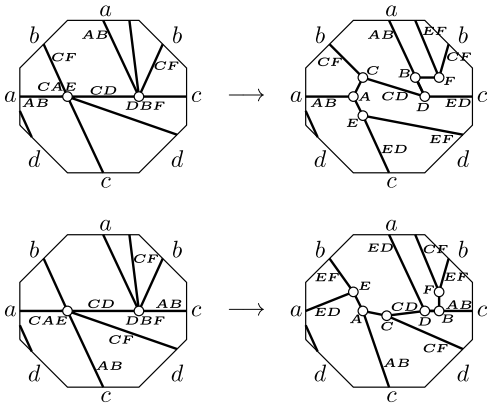

Fig. 9. $\Theta_5^{\#3}$ with central edge *CD*.

of $\Theta_5^{\#2}$ in Fig. 1) is expanded to the path $[D, B, F]$, edges CD, ED must be consecutive because they are both incident on D; and CF, EF must be consecutive because they are both incident on F. One can see that it is not possible to satisfy these conditions, for any labelling of the edges incident on u (CAE). An example of one of the cases is illustrated in Fig. 8. The other cases are similar. (All the cases can be easily considered by fixing one of the five edges to be AB.) □

Lemma 11. *Up to isomorphism, there are at most three extensions of* $\Theta_5^{\#3}$ *to* $K_{3,3}$.

Proof. Without loss of generality, the central edge of $\Theta_5^{\#3}$ can be taken as one of CD or AB.

Case *CD*.

Amongst the edges incident on vertex CAE in Fig. 9, edges CD and CF must be consecutive. This gives two choices for CF, which are shown in Fig. 9 (on the left). Also, edges ED and EF must be consecutive. The remaining edge must be AB. However, at vertex DBF, edges DC and DE must be consecutive, as must FC and FE. This forces the rest of the labelling of the edges, which then extends to an embedding of $K_{3,3}$ in two possible ways.

Case *AB*.

Refer to Figs. 10 and 11. Edges EF and ED must be consecutive at vertex CAE, and also edges CF and CD. At vertex DBF, edges CF and EF must be consecutive, as must edges CD and ED. This leads to four extensions to $K_{3,3}$. However, it is easy to see from the diagram in Fig. 11 that all four are isomorphic, giving only one extension with central edge AB. □

Theorem 12. *Up to isomorphism, there is a unique 2-cell embedding of* $K_{3,3}$ *on the double torus.*

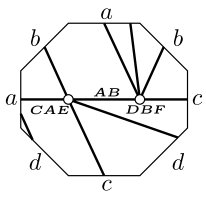

Fig. 10. $\Theta_5^{\#3}$ with central edge AB.

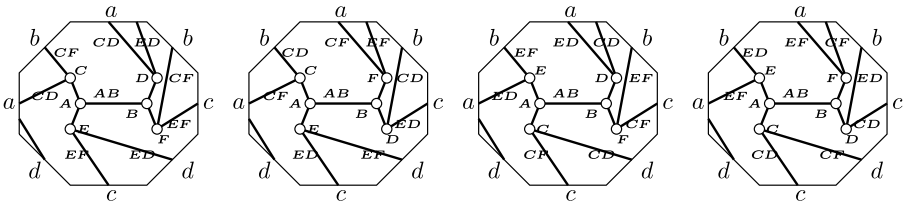

Fig. 11. Extensions of $\Theta_5^{\#3}$ to $K_{3,3}$ with central edge AB.

Proof. There are four labelled 2-cell embeddings found in Lemma 9 and three more in Lemma 11. In order to compare these for isomorphism, we can reduce the problem to digraph isomorphism as follows. Each labelled embedding can be described by a rotation system in a unique way, i.e., there is a one-to-one correspondence between the embeddings and their rotation systems (see Introduction and [8] for more details). For example, the rotation system of the left embedding in Fig. 7 can be represented as

$A : (B, C, E)$
$B : (A, F, D)$
$C : (A, F, D)$
$D : (B, E, C)$
$E : (A, F, D)$
$F : (B, C, E)$

We convert an embedding to its medial digraph — each edge of the embedding is subdivided with a new vertex, and a directed cycle is drawn around each vertex using the subdividing vertices, according to the cyclic order and direction in the rotation system. Isomorphic embeddings produce isomorphic medial digraphs, and vice-versa (see [3,8] for more details). By constructing the medial digraphs, and comparing them for isomorphism using graph isomorphism software (e.g. see [7]), we find that all the embeddings of $K_{3,3}$ found above are isomorphic.

Alternatively, we can show all these isomorphisms explicitly. Consider the four embeddings in Fig. 7 ordered from left to right. It is possible to see that these four embeddings are isomorphic as follows: permutation $(AB)(CD)(EF)$ is an isomorphism between the first two embeddings, permutation $(D)(E)(AF)(BC)$ is an isomorphism between the first and the third embeddings (reversing the rotations), and permutation $(C)(F)(AD)(BE)$ is an isomorphism between the second and the fourth embeddings (reversing the rotations).

Then, permutation $(A)(C)(BE)(DF)$ is an isomorphism between the two embeddings of $K_{3,3}$ in Fig. 9 (reversing the rotations). The left embedding in Fig. 11 is the same as the lower embedding of $K_{3,3}$ in Fig. 9, i.e. the identity permutation $(A)(B)(C)(D)(E)(F)$ provides an isomorphism in this case. Finally, permutation $(B)(CE)(AFD)$ is an isomorphism between the left embedding in Fig. 7 and the upper embedding of $K_{3,3}$ in Fig. 9. This completes a theoretical proof "by hand" that all seven labelled embeddings of $K_{3,3}$ found in Lemmas 9 and 11 are isomorphic. The unique 2-cell embedding of $K_{3,3}$ is shown in Fig. 12. □

It is easy to see that the embedding in Fig. 12 is non-orientable: the permutation $(1)(4)(26)(35)$ of vertices of $K_{3,3}$, which is an automorphism of $K_{3,3}$, maps the rotations to their reversals, implying the non-orientability.

4. Hyperbolic tilings

It is well known (see [15]) that the torus has symbolic representations $a^+b^+a^-b^-$ and $a^+b^+c^+a^-b^-c^-$, which also represent tilings of the Euclidean plane by rectangles and by regular hexagons, respectively. In the tiling by rectangles, four rectangles meet at each vertex. In the tiling by hexagons, three hexagons meet at each vertex. The corresponding translation groups of the plane map rectangles to rectangles, and hexagons to hexagons. Any graph embedding on the torus which has exactly one face, and the face is equivalent to an open disc, provides a polygonal representation of the

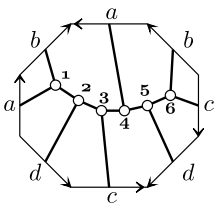

Fig. 12. The unique 2-cell embedding of $K_{3,3}$ on the double torus.

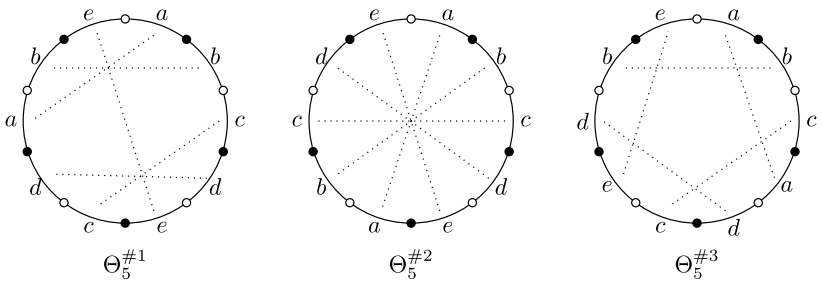

Fig. 13. Three 10-gons representing the double torus as a fundamental region of the hyperbolic plane.

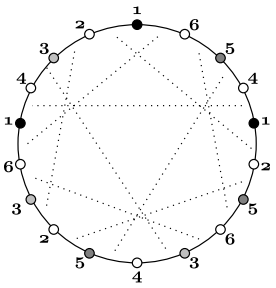

Fig. 14. The 18-gon representation of the double torus derived from $K_{3,3}$.

torus. By Euler's formula, the number of vertices and edges then satisfy $n+1-\varepsilon = 0$, so that $\varepsilon = n+1$. Since we require the minimum degree to be at least three, this limits the possible graphs. We must then have $n \leq 2$, from which it follows that the rectangle and hexagon are the only one-polygon representations of the torus.

With the double torus, there are many more possibilities for such one-face embeddings. The standard representation $a^+b^+a^-b^-c^+d^+c^-d^-$ of the double torus produces a tiling of the hyperbolic plane by regular octagons, in which eight octagons meet at each vertex. The 2-cell embeddings of Θ_5 and $K_{3,3}$ produce additional tilings of the hyperbolic plane. The three embeddings of Θ_5 produce tilings by regular 10-gons, i.e. polygons with 10 sides. One has fundamental region $a^+b^+c^+d^+e^+c^-d^-a^-b^-e^-$, the second has fundamental region $a^+b^+c^+d^+e^+a^-b^-c^-d^-e^-$, and the third has fundamental region $a^+b^+c^+a^-d^+c^-e^+d^-b^-e^-$. In each case five 10-gons meet at each vertex. The polygons of the fundamental regions determined by the embeddings of Θ_5 are shown in Fig. 13. Dotted lines are used to show the pairing of edges of the 10-gons. The polygon boundaries are traversed in a clockwise direction, such that for each pair of corresponding edges, the orientations of the two edges are opposite.

$K_{3,3}$ produces a tiling of the hyperbolic plane by regular 18-gons, i.e., polygons with 18 sides, with three 18-gons meeting at each vertex. It gives a polygonal representation $a^+b^+c^+d^+e^+f^+b^-g^+h^+c^-f^-i^+g^-a^-d^-h^-i^-e^-$ of the double torus. The edges of the fundamental polygon are the nine edges of $K_{3,3}$, each one appearing twice on the polygon boundary. This is illustrated in Fig. 14, where dotted lines show the pairing of edges of the polygon.

Euler's formula for the double torus and a one-face embedding gives $\varepsilon = n+3$. Since the minimum degree is required to be at least three, this gives $2\varepsilon \geq 3n$, or $2(n+3) \geq 3n$, giving $n \leq 6$. There are a number of graphs satisfying this condition. Each one will give a number of representations of the double torus as a fundamental region of the hyperbolic plane. We use some of them to find the 2-cell embeddings of K_5 on the double torus in the next section.

5. K_5 on the double torus

In this section, we find the distinct 2-cell embeddings of K_5 using a number of intermediate graphs. They are related to $K_{3,3}$ and Θ_5, and can be used as building blocks for 2-cell embeddings of various other graphs.

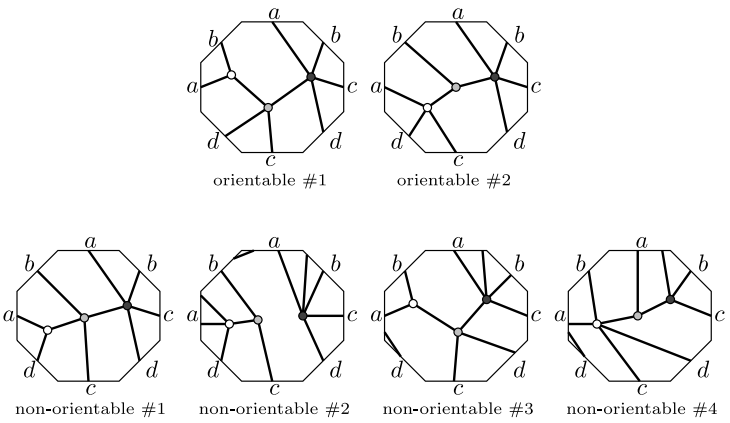

Fig. 15. The six inequivalent 2-cell embeddings of $T_{1,2,3}$.

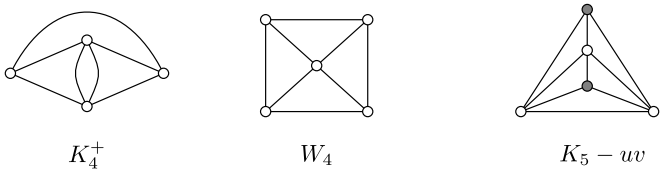

Fig. 16. The graphs K_4^+, W_4, and $K_5 - uv$.

The double torus is an orientable surface. If the rotations of an embedding are all reversed, an equivalent, but possibly non-isomorphic, embedding results. Two such embeddings will be considered as *equivalent*. As before, an embedding G^τ whose reversal is isomorphic to G^τ is said to be *non-orientable*. But if the reversal is non-isomorphic to G^τ, then the embedding is said to be *orientable*.

Let $T_{i,j,k}$ denote the graph of a triangle in which one edge has multiplicity i, one edge has multiplicity j, and the third edge has multiplicity k. For example, $T_{1,1,1} = K_3$. $T_{i,j,k}$ has $i+j+k$ edges, so that a 2-cell embedding of $T_{i,j,k}$ on the double torus has $f = i+j+k-5$ faces. The most interesting case is when $f = 1$, for then the embedding must be a 2-cell embedding, with no digon faces. We look at $T_{1,2,3}$.

Theorem 13. *Up to equivalence, $T_{1,2,3}$ has two orientable 2-cell embeddings, and four non-orientable 2-cell embeddings on the double torus.*

Proof. Let uv be the edge of $T_{1,2,3}$ with multiplicity one. Then $T_{1,2,3} \cdot uv \cong \Theta_5$. By Lemma 6, a 2-cell embedding of $T_{1,2,3}$ can be contracted to a 2-cell embedding of Θ_5, because uv is not part of a digon, and because the facial boundary of the unique face of $T_{1,2,3}$ is not a triangle. Consequently every embedding of $T_{1,2,3}$ can be constructed by reversing the edge contraction. Each vertex of Θ_5 has degree five.

By Corollary 5, the two vertices of $\Theta_5^{\#1}$ or $\Theta_5^{\#2}$ are equivalent, so that there are just five ways of reversing the edge contraction for each of these embeddings (because each vertex has degree five and any three edges must be consecutive in the resulting rotation). For embedding $\Theta_5^{\#3}$, there are 10 ways of reversing the edge contraction – five for each vertex. Comparison of the resulting 20 embeddings of $T_{1,2,3}$ shows that eight are non-isomorphic. However, reversing the rotations shows that four are non-orientable, and the other four fall into two pairs of equivalent orientable embeddings. The six inequivalent embeddings are shown in Fig. 15. □

Denote by K_4^+ the graph obtained from K_4 by doubling one edge. Euler's formula tells us that a 2-cell embedding of K_4^+ on the double torus has just one face.

Theorem 14. *Up to equivalence, K_4^+ has two orientable 2-cell embeddings, and three non-orientable 2-cell embeddings on the double torus.*

Proof. Consider a 2-cell embedding of K_4^+. It has just one face, so that there is no digon or triangular face. By Lemma 6 and by Fig. 16, we see that every 2-cell embedding of K_4^+ has four edges whose contraction results in a 2-cell embedding of $T_{1,2,3}$. The edge that was contracted maps to the unique vertex of $T_{1,2,3}$ of degree five. Consequently, every 2-cell embedding of K_4^+ can be obtained from some 2-cell embedding of $T_{1,2,3}$ by reversing an edge-contraction using the vertex

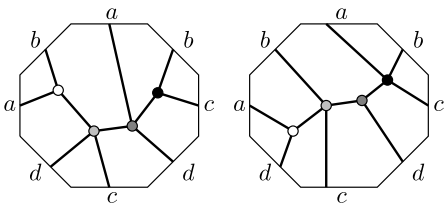

Fig. 17. The two inequivalent orientable 2-cell embeddings of K_4^+.

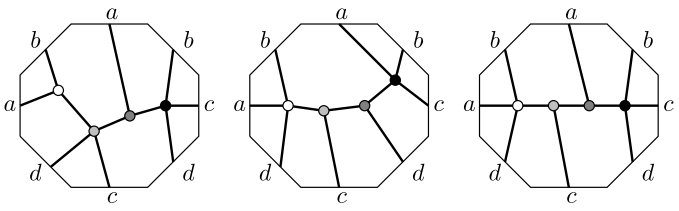

Fig. 18. The three inequivalent non-orientable 2-cell embeddings of K_4^+.

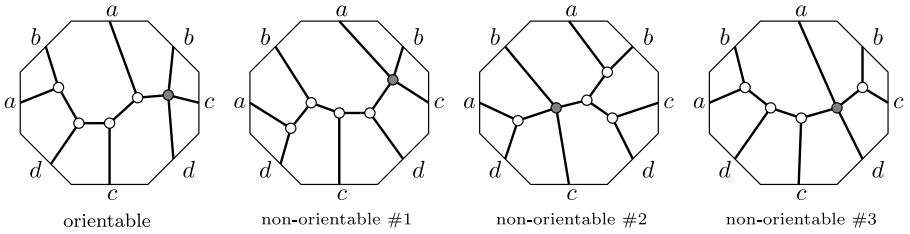

Fig. 19. The four inequivalent 2-cell embeddings of W_4.

of degree five. Starting from the embeddings of Fig. 15, there are at most five ways of splitting the vertex of degree five into vertices of degree three and four. The vertex must be split so that the triple and double edge result in one double edge, and various single edges. There are at most 30 embeddings that can be obtained like this. Using isomorphism testing software to distinguish them, we find that there are two orientable embeddings and three non-orientable embeddings, shown in Figs. 17 and 18. □

Consider now a 2-cell embedding of the wheel graph W_4, shown in Fig. 16.

Theorem 15. *Up to equivalence, W_4 has one orientable 2-cell embedding, and three non-orientable 2-cell embeddings on the double torus.*

Proof. Consider a 2-cell embedding of W_4. By Euler's formula, it has just one face. From Fig. 16, we see that contracting any one of the four "peripheral" edges results in K_4^+. By Lemma 6, this will be a 2-cell embedding of K_4^+. Consequently, every 2-cell embedding of W_4 can be obtained from a 2-cell embedding of K_4^+. The contracted edge maps onto one of the vertices of K_4^+ of degree four. Using the five embeddings of K_4^+ given by Theorem 14, we split each of the vertices of degree four in all possible ways that result in W_4. Then using isomorphism testing software to distinguish the resulting embeddings, we find that there is one orientable embedding and three non-orientable embeddings. They are shown in Fig. 19. □

We now turn to K_5.

Theorem 16. *Up to equivalence, K_5 has* 14 *orientable and* 17 *non-orientable 2-cell embeddings on the double torus.*

Proof. A 2-cell embedding of K_5 on the double torus has three faces. Therefore in every 2-cell embedding, there is at least one edge uv that has different faces on its two sides. If we delete this edge, we obtain a 2-cell embedding of $K_5 - uv$, an embedding with two faces. Therefore $K_5 - uv$ also has at least one edge with different faces on its two sides. By removing such an edge, we obtain a 2-cell embedding of a graph with $f = 1$. $K_5 - uv$ is shown in Fig. 16, where u and v are shaded grey. It consists of a triangle (x, y, z), with vertices u and v both adjacent to each of $\{x, y, z\}$. Consequently it has just two kinds of edges — those on the triangle (x, y, z), and those incident on u or v. If an edge of the triangle (x, y, z) is deleted,

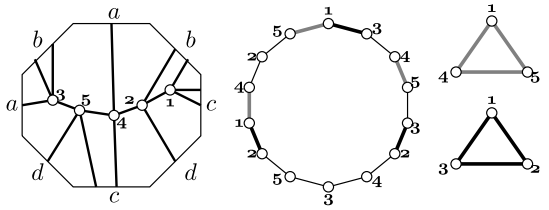

Fig. 20. An orientable embedding of K_5 with the trivial automorphism group.

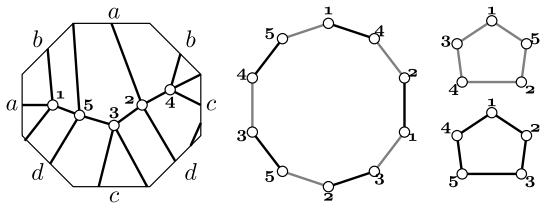

Fig. 21. The non-orientable embedding of K_5 with the automorphism group of order 5.

the result is the wheel graph W_4. If an edge incident on u or v is deleted, the resulting graph is homeomorphic to K_4^+, having a vertex of degree two. Either case is possible.

We start with the 2-cell embeddings of W_4 and K_4^+. With W_4, we add an edge between two non-adjacent vertices in all possible ways, to obtain a 2-cell embedding of $K_5 - uv$. There are many ways of doing this, because a 2-cell embedding of W_4 has a single facial cycle of length 16. Each vertex of degree three appears three times on the facial cycle, so that there are 18 ways of adding an edge to each embedding of W_4. This gives 72 embeddings of $K_5 - uv$ derived from W_4.

With K_4^+, we subdivide one of the pair of double edges with a new vertex x, and then add an edge xu, where u is a vertex of degree three. There are 24 ways to do this for each 2-cell embedding of K_4^+, giving 120 more embeddings of $K_5 - uv$.

The embeddings of $K_5 - uv$ are then distinguished with isomorphism testing software, giving 60 non-isomorphic embeddings in total, which reduces to 21 orientable and 18 non-orientable 2-cell embeddings of $K_5 - uv$. Finally, the deleted edge uv is added to each embedding of $K_5 - uv$ in all possible ways. There can be numerous ways to add uv to each embedding. The result is 45 non-isomorphic embeddings in total, which reduces to 14 orientable and 17 non-orientable 2-cell embeddings of K_5. □

The addition of edges to K_4^+, W_4, and $K_5 - uv$ in all possible ways in Theorem 16 was done by using a computer program. A list of rotation systems for the resulting 31 inequivalent 2-cell embeddings of K_5 is given in Appendix A. Most of the 31 embeddings (27) have an automorphism group of order one (for example, see Fig. 20). There is one embedding with a group of order five, two with a group of order four, and one with a group of order two.

Several of the embeddings are interesting. One of the non-orientable embeddings has an automorphism group of order five. It is shown in Fig. 21, together with its three facial cycles. Its automorphism group is generated by the permutation $(1, 2, 3, 5, 4)$. The three faces determine a decomposition of the double torus, as well as a tiling of the hyperbolic plane by decagons and pentagons, in which two pentagons and two decagons meet at each corner.

The 10-gon representations of Fig. 13 for the double torus are often more suitable for drawing embeddings of K_5 than the standard octagon form of the double torus. Fig. 22 shows a drawing of K_5 on two of the 10-gon representations. As can be seen from the drawing, these embeddings have an automorphism group of order five. They are isomorphic embeddings, although this is not evident from the diagram.

6. Conclusion

This paper provides a method for constructing all distinct 2-cell embeddings of various graphs on the double torus, and presents all the 2-cell embeddings of fundamental non-planar graphs $K_{3,3}$ and K_5 on the orientable surfaces, as a complement to their well-known toroidal embeddings. From Euler's formula, the maximum orientable genus of $K_{3,3}$ is two, the maximum orientable genus of K_5 is three, and the 2-cell embeddings of $K_{3,3}$ on the double torus and K_5 on the triple torus have a single face. Therefore, $K_{3,3}$ has orientable genus spectrum $\{1, 2\}$, and K_5 has orientable genus spectrum $\{1, 2, 3\}$.

By reconstructing embeddings from graph minors, we obtain the unique 2-cell embedding of $K_{3,3}$ and all distinct 2-cell embeddings of K_5 on the double torus. The 2-cell embeddings of K_5 on the triple torus are obtained by using an exhaustive computer search of rotation systems. Fig. 12 shows the unique embedding of $K_{3,3}$ on the double torus, Appendix A provides all the 2-cell embeddings of K_5 on the double torus (represented by their rotation systems), and Appendix B provides

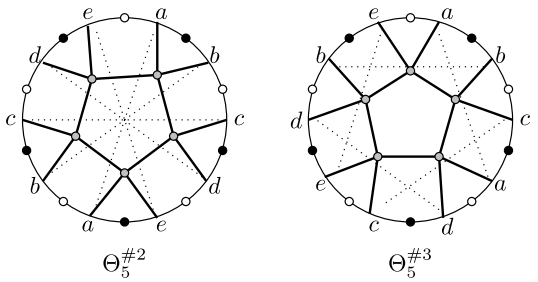

Fig. 22. Embeddings of K_5 on two 10-gon representations of the double torus.

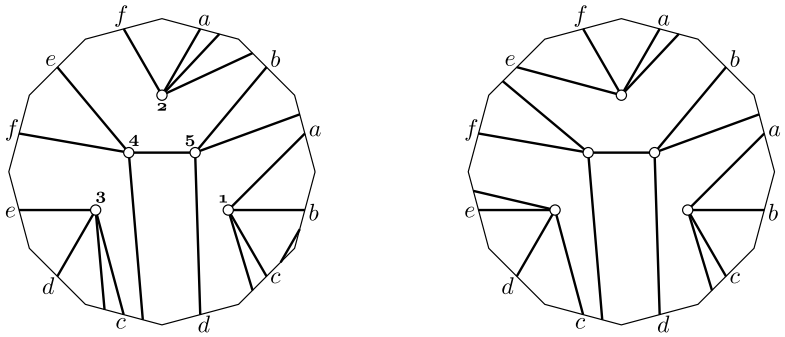

Fig. 23. Orientable (K5#a) and non-orientable (K5#l) 2-cell embeddings of K_5 on the triple torus.

all the rotation systems for different 2-cell embeddings of K_5 on the triple torus. Thus, $K_{3,3}$ has $3(=2+1)$ and K_5 has $50(=6+31+13)$ inequivalent 2-cell embeddings on orientable surfaces in total. In Appendix C, we report some corrections to previous computational results from [3] for embeddings of small vertex-transitive graphs (and $K_{3,4}$, $K_{3,5}$, $K_{3,6}$) on the torus — these corrections result from a corrected bug in computer code (spotted by Professor William Dickinson, Grand Valley State University). Notice that, in the table of Appendix C, the unique embeddings of vertex-transitive graphs K_7, $\sim(4K_2)$, $\sim(3K_3)$, and $\sim C_9$ on the torus are among the 21 irreducible triangulations of the torus explicitly shown in [10] (see embeddings T^1, T^2, T^7, and T^6 in Table 1 of paper [10], respectively).

Notice that the description of rotation systems in Appendix A allows a drawing of the embedding on the double torus to be constructed from its rotation system. However, in general, it is a non-trivial task to find a drawing of a graph on a polygonal representation of a surface from its rotation system. An ad-hoc approach has been used to draw two of the rotation systems from Appendix B for embeddings of K_5 on the triple torus shown in Fig. 23. The reader is encouraged to draw the other 11 embeddings from Appendix B. It would be interesting to find a constructive method to obtain all 2-cell embeddings of K_5 on the triple torus.

This paper also provides a number of different representations of the double torus and several examples of drawn 2-cell embeddings, e.g. a symmetric non-orientable embedding of K_5 (Figs. 21 and 22), an orientable embedding of K_5 with the trivial automorphism group (Fig. 20) on the double torus, two embeddings of K_5 on the triple torus (having one face, Fig. 23). Different representations of the double torus can be used, for example, to have symmetric drawings of the embeddings (Fig. 22) or to solve geometric packing problems like in Brandt et al. [1]. For future research, it would be interesting to describe more precisely and obtain all polygonal representations of the double and triple tori. Possibly some classic results to efficiently solve *NP*-hard optimization problems for planar graphs (e.g., see [4]) can be extended to non-planar graphs by studying their embeddings on surfaces of higher genus.

Since the multi-graph Θ_5 and its embeddings on the double torus play a crucial role in obtaining all the embeddings of $K_{3,3}$ and K_5 on this surface (similarly to the unique embedding of Θ_3 on the torus), we ask the following question for future work.

Open problem: How many distinct embeddings does Θ_{2g+1} have on the orientable surface of genus g, and how can they be obtained?

By Euler's formula, these embeddings will have a single face. When $g = 1$, there is one embedding. When $g = 2$, there are three embeddings.

Acknowledgements

We are grateful to the anonymous reviewers for carefully reading the original manuscript and providing useful and interesting comments.

Appendices

Rotation systems for all inequivalent embeddings of K_5 on the double and triple tori are given in Appendices A and B, and a corrected table for the embeddings of small vertex-transitive graphs on the torus from [3] is shown in Appendix C. The rotation for vertex $k \in \{1, 2, 3, 4, 5\}$ is indicated by $-k$, followed by the cyclic list of adjacent vertices. The orientable embeddings are indicated by "or", the non-orientable by "non".

Appendix A

Rotation systems for the 31 inequivalent 2-cell embeddings of K_5 on the double torus are listed below. The numbers in square brackets indicate the edge number, followed by a list of which sides of the fundamental octagon region are cut by the edge, so that a drawing of the corresponding embedding can be reconstructed from the rotation system.

K5#01 (or)
-1 5 [1 0 0 0 0] 4 [2 0 0 0 0] 2 [3 −3 0 0 0] 3 [4 −3 2 0 0]
-2 3 [5 2 0 0 0] 1 [3 3 0 0 0] 5 [6 4 0 0 0] 4 [7 0 0 0 0]
-3 4 [8 −1 0 0 0] 1 [4 −2 3 0 0] 2 [5 −2 0 0 0] 5 [9 0 0 0 0]
-4 2 [7 0 0 0 0] 1 [2 0 0 0 0] 5 [10 0 0 0 0] 3 [8 1 0 0 0]
-5 1 [1 0 0 0 0] 2 [6 −4 0 0 0] 3 [9 0 0 0 0] 4 [10 0 0 0 0]

K5#02 (or)
-1 5 [1 0 0 0 0] 4 [2 0 0 0 0] 2 [3 −3 0 0 0] 3 [4 −3 2 −1 0]
-2 3 [5 2 0 0 0] 1 [3 3 0 0 0] 5 [6 4 0 0 0] 4 [7 0 0 0 0]
-3 5 [8 0 0 0 0] 4 [9 −1 0 0 0] 2 [5 −2 0 0 0] 1 [4 1 −2 3 0]
-4 2 [7 0 0 0 0] 1 [2 0 0 0 0] 5 [10 0 0 0 0] 3 [9 1 0 0 0]
-5 1 [1 0 0 0 0] 2 [6 −4 0 0 0] 3 [8 0 0 0 0] 4 [10 0 0 0 0]

K5#03 (or)
-1 5 [1 0 0 0 0] 4 [2 0 0 0 0] 2 [3 −3 0 0 0] 3 [4 −3 2 −1 0]
-2 3 [5 2 0 0 0] 1 [3 3 0 0 0] 5 [6 4 0 0 0] 4 [7 0 0 0 0]
-3 5 [8 0 0 0 0] 4 [9 −1 0 0 0] 2 [5 −2 0 0 0] 1 [4 1 −2 3 0]
-4 2 [7 0 0 0 0] 1 [2 0 0 0 0] 3 [9 1 0 0 0] 5 [10 1 0 0 0]
-5 1 [1 0 0 0 0] 2 [6 −4 0 0 0] 4 [10 −1 0 0 0] 3 [8 0 0 0 0]

K5#04 (or)
-1 5 [1 0 0 0 0] 4 [2 0 0 0 0] 2 [3 −3 0 0 0] 3 [4 −3 2 −1 0]
-2 3 [5 2 0 0 0] 1 [3 3 0 0 0] 5 [6 4 0 0 0] 4 [7 0 0 0 0]
-3 5 [8 0 0 0 0] 4 [9 −1 0 0 0] 2 [5 −2 0 0 0] 1 [4 1 −2 3 0]
-4 5 [10 −3 4 0 0] 1 [2 0 0 0 0] 3 [9 1 0 0 0] 2 [7 0 0 0 0]
-5 1 [1 0 0 0 0] 2 [6 −4 0 0 0] 4 [10 −4 3 0 0] 3 [8 0 0 0 0]

K5#05 (or)
-1 5 [1 0 0 0 0] 4 [2 0 0 0 0] 2 [3 −3 0 0 0] 3 [4 −4 −3 4 0]
-2 3 [5 2 0 0 0] 1 [3 3 0 0 0] 5 [6 4 0 0 0] 4 [7 0 0 0 0]
-3 1 [4 −4 3 4 0] 4 [8 −1 0 0 0] 2 [5 −2 0 0 0] 5 [9 0 0 0 0]
-4 2 [7 0 0 0 0] 1 [2 0 0 0 0] 5 [10 0 0 0 0] 3 [8 1 0 0 0]
-5 1 [1 0 0 0 0] 2 [6 −4 0 0 0] 3 [9 0 0 0 0] 4 [10 0 0 0 0]

K5#06 (or)
-1 5 [1 0 0 0 0] 4 [2 0 0 0 0] 2 [3 −3 0 0 0] 3 [4 −4 −3 4 0]
-2 3 [5 2 0 0 0] 1 [3 3 0 0 0] 5 [6 4 0 0 0] 4 [7 0 0 0 0]
-3 1 [4 −4 3 4 0] 4 [8 −1 0 0 0] 2 [5 −2 0 0 0] 5 [9 0 0 0 0]
-4 2 [7 0 0 0 0] 1 [2 0 0 0 0] 3 [8 1 0 0 0] 5 [10 2 0 0 0]
-5 1 [1 0 0 0 0] 2 [6 −4 0 0 0] 3 [9 0 0 0 0] 4 [10 −2 0 0 0]

K5#07 (or)
-1 3 [1 0 0 0 0] 4 [2 0 0 0 0] 5 [3 −3 0 0 0] 2 [4 −4 0 0 0]
-2 3 [5 1 0 0 0] 5 [6 0 0 0 0] 1 [4 4 0 0 0] 4 [7 0 0 0 0]
-3 2 [5 −1 0 0 0] 4 [8 −1 0 0 0] 5 [9 −2 0 0 0] 1 [1 0 0 0 0]
-4 2 [7 0 0 0 0] 1 [2 0 0 0 0] 5 [10 1 −2 0 0] 3 [8 1 0 0 0]
-5 2 [6 0 0 0 0] 3 [9 2 0 0 0] 4 [10 2 −1 0 0] 1 [3 3 0 0 0]

K5#08 (or)
-1 3 [1 0 0 0 0] 4 [2 0 0 0 0] 5 [3 −3 0 0 0] 2 [4 −4 0 0 0]
-2 3 [5 1 0 0 0] 5 [6 0 0 0 0] 1 [4 4 0 0 0] 4 [7 0 0 0 0]

-3 2 [5 −1 0 0 0] 4 [8 −1 0 0 0] 5 [9 −2 0 0 0] 1 [1 0 0 0 0]
-4 5 [10 −3 4 −1 0] 1 [2 0 0 0 0] 3 [8 1 0 0 0] 2 [7 0 0 0 0]
-5 4 [10 1 −4 3 0] 3 [9 2 0 0 0] 1 [3 3 0 0 0] 2 [6 0 0 0 0]

K5#09 (or)
-1 3 [1 0 0 0 0] 4 [2 0 0 0 0] 5 [3 −3 0 0 0] 2 [4 −4 0 0 0]
-2 3 [5 2 1 0 0] 5 [6 0 0 0 0] 1 [4 4 0 0 0] 4 [7 0 0 0 0]
-3 4 [8 −1 0 0 0] 2 [5 −1 −2 0 0] 5 [9 −2 0 0 0] 1 [1 0 0 0 0]
-4 2 [7 0 0 0 0] 1 [2 0 0 0 0] 5 [10 −2 0 0 0] 3 [8 1 0 0 0]
-5 4 [10 2 0 0 0] 3 [9 2 0 0 0] 1 [3 3 0 0 0] 2 [6 0 0 0 0]

K5#10 (or)
-1 3 [1 0 0 0 0] 4 [2 0 0 0 0] 5 [3 −3 0 0 0] 2 [4 −4 0 0 0]
-2 3 [5 2 1 0 0] 5 [6 0 0 0 0] 1 [4 4 0 0 0] 4 [7 0 0 0 0]
-3 4 [8 −1 0 0 0] 2 [5 −1 −2 0 0] 5 [9 −2 0 0 0] 1 [1 0 0 0 0]
-4 2 [7 0 0 0 0] 1 [2 0 0 0 0] 3 [8 1 0 0 0] 5 [10 2 1 −2 0]
-5 2 [6 0 0 0 0] 3 [9 2 0 0 0] 4 [10 2 −1 −2 0] 1 [3 3 0 0 0]

K5#11 (or)
-1 3 [1 0 0 0 0] 4 [2 0 0 0 0] 5 [3 −3 0 0 0] 2 [4 −4 0 0 0]
-2 3 [5 2 0 0 0] 5 [6 0 0 0 0] 1 [4 4 0 0 0] 4 [7 0 0 0 0]
-3 1 [1 0 0 0 0] 4 [8 −1 0 0 0] 5 [9 −2 0 0 0] 2 [5 −2 0 0 0]
-4 5 [10 4 −3 0 0] 1 [2 0 0 0 0] 3 [8 1 0 0 0] 2 [7 0 0 0 0]
-5 2 [6 0 0 0 0] 3 [9 2 0 0 0] 4 [10 3 −4 0 0] 1 [3 3 0 0 0]

K5#12 (or)
-1 3 [1 0 0 0 0] 4 [2 0 0 0 0] 5 [3 −3 0 0 0] 2 [4 −4 0 0 0]
-2 5 [5 0 0 0 0] 3 [6 4 0 0 0] 1 [4 4 0 0 0] 4 [7 0 0 0 0]
-3 2 [6 −4 0 0 0] 4 [8 −1 0 0 0] 5 [9 −2 0 0 0] 1 [1 0 0 0 0]
-4 2 [7 0 0 0 0] 1 [2 0 0 0 0] 5 [10 −2 0 0 0] 3 [8 1 0 0 0]
-5 4 [10 2 0 0 0] 3 [9 2 0 0 0] 1 [3 3 0 0 0] 2 [5 0 0 0 0]

K5#13 (or)
-1 3 [1 0 0 0 0] 4 [2 0 0 0 0] 5 [3 −3 0 0 0] 2 [4 −4 0 0 0]
-2 4 [5 0 0 0 0] 5 [6 0 0 0 0] 1 [4 4 0 0 0] 3 [7 4 −3 2 0]
-3 1 [1 0 0 0 0] 4 [8 −1 0 0 0] 2 [7 −2 3 −4 0] 5 [9 −2 0 0 0]
-4 2 [5 0 0 0 0] 1 [2 0 0 0 0] 3 [8 1 0 0 0] 5 [10 0 0 0 0]
-5 4 [10 0 0 0 0] 3 [9 2 0 0 0] 1 [3 3 0 0 0] 2 [6 0 0 0 0]

K5#14 (or)
-1 5 [1 0 0 0 0] 2 [2 −3 0 0 0] 3 [3 0 0 0 0] 4 [4 −2 0 0 0]
-2 3 [5 4 0 0 0] 5 [6 0 0 0 0] 1 [2 3 0 0 0] 4 [7 4 −1 0 0]
-3 2 [5 −4 0 0 0] 4 [8 −1 0 0 0] 5 [9 −1 0 0 0] 1 [3 0 0 0 0]
-4 2 [7 1 −4 0 0] 1 [4 2 0 0 0] 5 [10 0 0 0 0] 3 [8 1 0 0 0]
-5 4 [10 0 0 0 0] 2 [6 0 0 0 0] 1 [1 0 0 0 0] 3 [9 1 0 0 0]

K5#15 (non)
-1 5 [1 0 0 0 0] 4 [2 0 0 0 0] 2 [3 −3 0 0 0] 3 [4 −3 2 −1 0]
-2 3 [5 2 0 0 0] 1 [3 3 0 0 0] 5 [6 4 0 0 0] 4 [7 0 0 0 0]
-3 5 [8 0 0 0 0] 4 [9 −1 0 0 0] 2 [5 −2 0 0 0] 1 [4 1 −2 3 0]
-4 2 [7 0 0 0 0] 1 [2 0 0 0 0] 3 [9 1 0 0 0] 5 [10 1 −4 3 4]
-5 4 [10 −4 −3 4 −1] 2 [6 −4 0 0 0] 3 [8 0 0 0 0] 1 [1 0 0 0 0]

K5#16 (non)
-1 5 [1 0 0 0 0] 4 [2 0 0 0 0] 2 [3 −3 0 0 0] 3 [4 −3 2 −1 0]
-2 3 [5 2 0 0 0] 1 [3 3 0 0 0] 5 [6 4 0 0 0] 4 [7 0 0 0 0]
-3 5 [8 0 0 0 0] 4 [9 −1 0 0 0] 2 [5 −2 0 0 0] 1 [4 1 −2 3 0]
-4 5 [10 4 0 0 0] 1 [2 0 0 0 0] 3 [9 1 0 0 0] 2 [7 0 0 0 0]
-5 4 [10 −4 0 0 0] 2 [6 −4 0 0 0] 3 [8 0 0 0 0] 1 [1 0 0 0 0]

K5#17 (non)
-1 3 [1 0 0 0 0] 4 [2 0 0 0 0] 5 [3 −3 0 0 0] 2 [4 −4 0 0 0]
-2 3 [5 1 0 0 0] 5 [6 0 0 0 0] 1 [4 4 0 0 0] 4 [7 0 0 0 0]
-3 2 [5 −1 0 0 0] 4 [8 −1 0 0 0] 5 [9 −2 0 0 0] 1 [1 0 0 0 0]
-4 5 [10 4 −3 0 0] 1 [2 0 0 0 0] 3 [8 1 0 0 0] 2 [7 0 0 0 0]

-5 2 [6 0 0 0 0] 3 [9 2 0 0 0] 4 [10 3 −4 0 0] 1 [3 3 0 0 0]

K5#18 (non)
-1 3 [1 0 0 0 0] 4 [2 0 0 0 0] 5 [3 −3 0 0 0] 2 [4 −4 0 0 0]
-2 3 [5 1 0 0 0] 5 [6 0 0 0 0] 1 [4 4 0 0 0] 4 [7 0 0 0 0]
-3 2 [5 −1 0 0 0] 4 [8 −1 0 0 0] 5 [9 −2 0 0 0] 1 [1 0 0 0 0]
-4 5 [10 −3 0 0 0] 1 [2 0 0 0 0] 3 [8 1 0 0 0] 2 [7 0 0 0 0]
-5 2 [6 0 0 0 0] 3 [9 2 0 0 0] 1 [3 3 0 0 0] 4 [10 3 0 0 0]

K5#19 (non)
-1 3 [1 0 0 0 0] 4 [2 0 0 0 0] 5 [3 −3 0 0 0] 2 [4 −4 0 0 0]
-2 3 [5 2 1 0 0] 5 [6 0 0 0 0] 1 [4 4 0 0 0] 4 [7 0 0 0 0]
-3 4 [8 −1 0 0 0] 2 [5 −1 −2 0 0] 5 [9 −2 0 0 0] 1 [1 0 0 0 0]
-4 2 [7 0 0 0 0] 1 [2 0 0 0 0] 3 [8 1 0 0 0] 5 [10 1 −4 0 0]
-5 2 [6 0 0 0 0] 3 [9 2 0 0 0] 1 [3 3 0 0 0] 4 [10 4 −1 0 0]

K5#20 (non)
-1 3 [1 0 0 0 0] 4 [2 0 0 0 0] 5 [3 −3 0 0 0] 2 [4 −4 0 0 0]
-2 3 [5 2 1 0 0] 5 [6 0 0 0 0] 1 [4 4 0 0 0] 4 [7 0 0 0 0]
-3 4 [8 −1 0 0 0] 2 [5 −1 −2 0 0] 5 [9 −2 0 0 0] 1 [1 0 0 0 0]
-4 5 [10 4 −3 0 0] 1 [2 0 0 0 0] 3 [8 1 0 0 0] 2 [7 0 0 0 0]
-5 2 [6 0 0 0 0] 3 [9 2 0 0 0] 4 [10 3 −4 0 0] 1 [3 3 0 0 0]

K5#21 (non)
-1 3 [1 0 0 0 0] 4 [2 0 0 0 0] 5 [3 −3 0 0 0] 2 [4 −4 0 0 0]
-2 3 [5 2 0 0 0] 5 [6 0 0 0 0] 1 [4 4 0 0 0] 4 [7 0 0 0 0]
-3 1 [1 0 0 0 0] 4 [8 −1 0 0 0] 5 [9 −2 0 0 0] 2 [5 −2 0 0 0]
-4 2 [7 0 0 0 0] 1 [2 0 0 0 0] 5 [10 1 −2 0 0] 3 [8 1 0 0 0]
-5 2 [6 0 0 0 0] 3 [9 2 0 0 0] 4 [10 2 −1 0 0] 1 [3 3 0 0 0]

K5#22 (non)
-1 3 [1 0 0 0 0] 4 [2 0 0 0 0] 5 [3 −3 0 0 0] 2 [4 −4 0 0 0]
-2 3 [5 2 0 0 0] 5 [6 0 0 0 0] 1 [4 4 0 0 0] 4 [7 0 0 0 0]
-3 1 [1 0 0 0 0] 4 [8 −1 0 0 0] 5 [9 −2 0 0 0] 2 [5 −2 0 0 0]
-4 2 [7 0 0 0 0] 1 [2 0 0 0 0] 3 [8 1 0 0 0] 5 [10 1 −4 0 0]
-5 2 [6 0 0 0 0] 3 [9 2 0 0 0] 1 [3 3 0 0 0] 4 [10 4 −1 0 0]

K5#23 (non)
-1 3 [1 0 0 0 0] 4 [2 0 0 0 0] 5 [3 −3 0 0 0] 2 [4 −4 0 0 0]
-2 4 [5 0 0 0 0] 5 [6 0 0 0 0] 1 [4 4 0 0 0] 3 [7 4 −3 2 0]
-3 1 [1 0 0 0 0] 4 [8 −1 0 0 0] 2 [7 −2 3 −4 0] 5 [9 −2 0 0 0]
-4 2 [5 0 0 0 0] 1 [2 0 0 0 0] 3 [8 1 0 0 0] 5 [10 1 −4 0 0]
-5 2 [6 0 0 0 0] 3 [9 2 0 0 0] 1 [3 3 0 0 0] 4 [10 4 −1 0 0]

K5#24 (non)
-1 4 [1 −4 0 0 0] 2 [2 −1 0 0 0] 5 [3 0 0 0 0] 3 [4 0 0 0 0]
-2 5 [5 2 0 0 0] 3 [6 3 0 0 0] 4 [7 0 0 0 0] 1 [2 1 0 0 0]
-3 5 [8 0 0 0 0] 4 [9 0 0 0 0] 2 [6 −3 0 0 0] 1 [4 0 0 0 0]
-4 2 [7 0 0 0 0] 1 [1 4 0 0 0] 5 [10 4 −3 2 0] 3 [9 0 0 0 0]
-5 4 [10 −2 3 −4 0] 2 [5 −2 0 0 0] 3 [8 0 0 0 0] 1 [3 0 0 0 0]

K5#25 (non)
-1 3 [1 −1 2 0 0] 2 [2 −1 0 0 0] 5 [3 0 0 0 0] 4 [4 −4 0 0 0]
-2 5 [5 2 0 0 0] 3 [6 3 0 0 0] 4 [7 0 0 0 0] 1 [2 1 0 0 0]
-3 1 [1 −2 1 0 0] 4 [8 0 0 0 0] 2 [6 −3 0 0 0] 5 [9 0 0 0 0]
-4 2 [7 0 0 0 0] 1 [4 4 0 0 0] 3 [8 0 0 0 0] 5 [10 1 −2 3 0]
-5 1 [3 0 0 0 0] 2 [5 −2 0 0 0] 3 [9 0 0 0 0] 4 [10 −3 2 −1 0]

K5#26 (non)
-1 2 [1 −1 0 0 0] 3 [2 −2 3 0 0] 5 [3 0 0 0 0] 4 [4 −4 0 0 0]
-2 5 [5 2 0 0 0] 3 [6 3 0 0 0] 4 [7 0 0 0 0] 1 [1 1 0 0 0]
-3 5 [8 0 0 0 0] 4 [9 0 0 0 0] 2 [6 −3 0 0 0] 1 [2 −3 2 0 0]

-4 2 [7 0 0 0 0] 1 [4 4 0 0 0] 5 [10 4 0 0 0] 3 [9 0 0 0 0]
-5 1 [3 0 0 0 0] 2 [5 −2 0 0 0] 3 [8 0 0 0 0] 4 [10 −4 0 0 0]

K5#27 (non)
-1 2 [1 −1 0 0 0] 3 [2 −2 3 0 0] 5 [3 0 0 0 0] 4 [4 −4 0 0 0]
-2 5 [5 2 0 0 0] 3 [6 3 0 0 0] 4 [7 0 0 0 0] 1 [1 1 0 0 0]
-3 5 [8 0 0 0 0] 4 [9 0 0 0 0] 2 [6 −3 0 0 0] 1 [2 −3 2 0 0]
-4 5 [10 3 4 0 0] 1 [4 4 0 0 0] 3 [9 0 0 0 0] 2 [7 0 0 0 0]
-5 1 [3 0 0 0 0] 2 [5 −2 0 0 0] 3 [8 0 0 0 0] 4 [10 −4 −3 0 0]

K5#28 (non)
-1 5 [1 0 0 0 0] 2 [2 −3 0 0 0] 3 [3 0 0 0 0] 4 [4 −2 0 0 0]
-2 3 [5 4 0 0 0] 5 [6 0 0 0 0] 1 [2 3 0 0 0] 4 [7 4 −1 0 0]
-3 2 [5 −4 0 0 0] 4 [8 −1 0 0 0] 5 [9 −2 3 −4 0] 1 [3 0 0 0 0]
-4 2 [7 1 −4 0 0] 1 [4 2 0 0 0] 5 [10 0 0 0 0] 3 [8 1 0 0 0]
-5 4 [10 0 0 0 0] 2 [6 0 0 0 0] 3 [9 4 −3 2 0] 1 [1 0 0 0 0]

K5#29 (non)
-1 2 [1 −1 0 0 0] 4 [2 −2 0 0 0] 5 [3 0 0 0 0] 3 [4 −4 3 0 0]
-2 4 [5 0 0 0 0] 5 [6 4 0 0 0] 3 [7 0 0 0 0] 1 [1 1 0 0 0]
-3 2 [7 0 0 0 0] 1 [4 −3 4 0 0] 4 [8 −3 0 0 0] 5 [9 0 0 0 0]
-4 2 [5 0 0 0 0] 1 [2 2 0 0 0] 5 [10 2 −1 0 0] 3 [8 3 0 0 0]
-5 4 [10 1 −2 0 0] 3 [9 0 0 0 0] 2 [6 −4 0 0 0] 1 [3 0 0 0 0]

K5#30 (non)
-1 2 [1 −1 0 0 0] 4 [2 −2 0 0 0] 5 [3 0 0 0 0] 3 [4 −1 2 0 0]
-2 4 [5 0 0 0 0] 5 [6 4 0 0 0] 3 [7 0 0 0 0] 1 [1 1 0 0 0]
-3 1 [4 −2 1 0 0] 2 [7 0 0 0 0] 4 [8 −3 0 0 0] 5 [9 0 0 0 0]
-4 2 [5 0 0 0 0] 1 [2 2 0 0 0] 5 [10 2 −1 −2 1] 3 [8 3 0 0 0]
-5 1 [3 0 0 0 0] 3 [9 0 0 0 0] 2 [6 −4 0 0 0] 4 [10 −1 2 1 −2]

K5#31 (non)
-1 3 [1 −1 0 0 0] 4 [2 −2 0 0 0] 5 [3 0 0 0 0] 2 [4 −1 0 0 0]
-2 4 [5 0 0 0 0] 5 [6 4 0 0 0] 3 [7 0 0 0 0] 1 [4 1 0 0 0]
-3 1 [1 1 0 0 0] 2 [7 0 0 0 0] 4 [8 −3 0 0 0] 5 [9 0 0 0 0]
-4 2 [5 0 0 0 0] 1 [2 2 0 0 0] 5 [10 2 −1 −2 1] 3 [8 3 0 0 0]
-5 1 [3 0 0 0 0] 3 [9 0 0 0 0] 2 [6 −4 0 0 0] 4 [10 −1 2 1 −2]

Appendix B

Rotation systems for the 13 inequivalent 2-cell embeddings of K_5 on the triple torus, 11 orientable and 2 non-orientable. Each embedding has exactly one face, with each vertex appearing four times and each edge appearing twice on its boundary. These were found by constructing all possible rotation systems for K_5 for any orientable genus, then selecting those with exactly one face, so that it is a rotation system for the triple torus. This method does not construct drawings of the embeddings.

K5#a (or)
-1 2 5 3 4
-2 1 5 3 4
-3 1 2 5 4
-4 1 2 3 5
-5 1 2 3 4

K5#b (or)
-1 2 4 3 5
-2 1 3 4 5
-3 1 2 5 4
-4 1 2 3 5
-5 1 2 3 4

K5#c (or)
-1 2 4 3 5
-2 1 3 4 5
-3 1 5 2 4
-4 1 2 5 3
-5 1 2 3 4

K5#d (or)
-1 2 4 5 3
-2 1 3 4 5
-3 1 5 2 4
-4 1 2 5 3
-5 1 2 3 4

K5#e (or)
-1 2 5 3 4
-2 1 4 5 3
-3 1 5 2 4
-4 1 2 5 3
-5 1 2 3 4

K5#f (or)
-1 2 5 4 3
-2 1 4 5 3
-3 1 5 2 4
-4 1 2 5 3
-5 1 2 3 4

K5#g (or)
-1 2 5 4 3
-2 1 5 3 4
-3 1 5 4 2
-4 1 2 5 3
-5 1 2 3 4

K5#h (or)
-1 2 3 4 5
-2 1 3 4 5
-3 1 5 4 2
-4 1 2 5 3
-5 1 2 3 4

K5#i (or)
-1 2 4 3 5
-2 1 3 4 5
-3 1 5 4 2
-4 1 2 5 3
-5 1 2 3 4

K5#j (or)
-1 2 5 4 3
-2 1 5 3 4
-3 1 2 5 4
-4 1 3 2 5
-5 1 2 3 4

K5#k (or)
-1 2 3 4 5
-2 1 5 4 3
-3 1 5 4 2
-4 1 3 2 5
-5 1 2 3 4

K5#l (non)
-1 2 3 4 5
-2 1 4 3 5
-3 1 2 5 4
-4 1 2 3 5
-5 1 2 3 4

K5#m (non)
-1 2 3 4 5
-2 1 5 4 3
-3 1 4 5 2
-4 1 3 2 5
-5 1 2 3 4

Appendix C

Erratum to [3]. Tables of torus embeddings of many small graphs appear in [3]. The software that generated the original embeddings missed several embeddings. The condition that controls the loop was incorrect, causing the loop to sometimes stop too soon. The corrected numbers of embeddings are shown in the following table. The graphs with corrected entries are marked with [*] in the last column. These are taken from http://www.combinatoire.ca/G&G/.

(And in the toroidal embedding K_5#1 of Figure 7 and Figure 1 of [3], the embedding is incorrectly marked as non-orientable.)

graph	n	ε	f	**#emb.**	**or.**	**non.**	**groups**
K_4	4	6	2	2	0	2	[24] 4^1, 3^1
K_5	5	10	5	6	3	3	[120] 20^1, 4^1, 2^3, 1^1 [*]
$K_{3,3}$	6	9	3	2	0	2	[72] 18^1, 2^1
3-Prism	6	9	3	5	0	5	[12] 6^1, 2^2, 1^2
Octahedron	6	12	6	17	4	13	[48] 12^1, 6^1, 4^3, 3^1, 2^6, 1^5
K_6	6	15	9	4	2	2	[720] 6^2, 2^1, 1^1
$K_{3,4}$	7	12	5	3	0	3	[144] 4^1, 3^1, 2^1
$\sim C_7 = C_7(2)$	7	14	7	28	23	5	[14] 14^1, 2^{14}, 1^{13}
K_7 [Δ]	7	21	14	1	1	0	[5040] 42^1
$K_{3,5}$	8	15	7	1	0	1	[720] 3^1
Cube $= C_4 \times K_2$	8	12	4	5	0	5	[48] 24^1, 8^2, 3^1, 2^1
C_8^+	8	12	4	5	1	4	[16] 2^4, 1^1[*]
$K_{4,4}$	8	16	8	2	0	2	[1152] 32^1, 16^1
$\sim C_8+ = C_8(2)$	8	16	8	37	20	17	[16] 16^1, 4^4, 2^{13}, 1^{19} [*]
$\sim$Cube	8	16	8	8	4	4	[48] 4^2, 2^5, 1^1
$\sim C_8$	8	20	12	10	10	0	[16] 2^7, 1^3 [*]
$\sim(2C_4)$	8	20	12	6	2	4	[128] 8^2, 4^2, 2^2 [*]
$\sim(4K_2)$ [Δ]	8	24	16	1	0	1	[384] 16^1
$K_{3,6}$	9	18	9	1	0	1	[4320] 18^1
$C_9(2)$	9	18	9	37	34	3	[18] 18^1, 6^1, 2^{19}, 1^{16} [*]
$C_9(3)$	9	18	9	6	4	2	[18] 18^1, 3^1, 2^3, 1^1 [*]
$K_3 \times K_3$ = Paley	9	18	9	7	3	4	[72] 36^1, 18^1, 4^1, 2^3, 1^1
$\sim(3K_3)$ [Δ]	9	27	18	1	0	1	[1296] 54^1
$\sim C_9$ [Δ]	9	27	18	1	1	0	[18] 18^1
Petersen	10	15	5	1	0	1	[120] 3^1
C_{10}^+	10	15	5	6	1	5	[20] 10^1, 2^4, 1^1
$C_5 \times K_2$ = 5-Prism	10	15	5	5	0	5	[20] 2^3, 1^2
$C_{10}(2)$	10	20	10	60	42	18	[20] 20^1, 4^3, 2^{23}, 1^{33}
$C_{10}(4)$	10	20	10	1	1	0	[320] 20^1
$\sim(K_5 \times K_2)$	10	20	10	1	1	0	[240] 40^1
$\sim C_{10}(2)$	10	25	15	1	0	1	[20] 10^1
$\sim C_{10}(4)$	10	25	15	4	4	0	[320] 10^1, 2^3
$\sim(C_5 \times K_2)$ [Δ]	10	30	20	1	1	0	[20] 20^1
$C_{11}(2)$	11	22	11	77	74	3	[22] 22^1, 2^{36}, 1^{40} [*]
$C_{11}(3)$	11	22	11	1	1	0	[22] 22^1
$\sim C_{11}(3)$ [Δ]	11	33	22	1	1	0	[22] 22^1
$C_{12}(5^+)$	12	18	6	3	1	2	[48] 12^1, 6^1, 2^1[*]
$C_6 \times K_2$ = 6-Prism	12	18	6	9	0	9	[24] 12^1, 4^2, 2^4, 1^2
C_{12}^+	12	18	6	7	1	6	[24] 6^1, 2^4, 1^2
trunc(K_4)	12	18	6	9	0	9	[24] 4^1, 3^1, 2^2, 1^5
$C_{12}(3^+, 6)$	12	24	12	1	0	1	[48] 24^1
$C_{12}(2)$	12	24	12	138	110	28	[24] 24^1, 8^1, 6^2, 4^4, 2^{45}, 1^{85} [*]
$C_{12}(3)$	12	24	12	1	1	0	[24] 24^1
$C_{12}(4)$	12	24	12	2	1	1	[24] 24^1, 4^1
$C_{12}(5)$	12	24	12	2	0	2	[768] 24^2 [*]
$C_{12}(5^+, 6)$	12	24	12	10	10	0	[48] 6^2, 2^6, 1^2
L(Cube)	12	24	12	16	1	15	[48] 24^1, 8^2, 4^1, 3^1, 2^3, 1^8 [*]
$C_4 \times C_3$	12	24	12	3	0	3	[48] 24^1, 4^1, 2^1 [*]

antip(trunc(K_4))	12	24	12	1	0	1	[24] 3^1
Icosahedron	12	30	18	12	5	7	[120] $3^1, 2^4, 1^7$
Octahedron $\times K_2$	12	30	18	1	0	1	[96] 12^1
$C_{12}(5, 6)$	12	30	18	8	5	3	[768] $12^1, 6^1, 4^1, 2^4, 1^1$
$C_{12}(2, 5+)$	12	30	18	1	1	0	[12] 12^1
$C_{12}(4, 5^+)$	12	30	18	1	1	0	[12] 12^1
$C_{12}(2, 3)$ [Δ]	12	36	24	1	1	0	[24] 24^1
$C_{12}(2, 5)$ [Δ]	12	36	24	1	0	1	[144] 72^1
$C_{12}(3, 4)$ [Δ]	12	36	24	1	1	0	[24] 24^1
$C_{12}(4, 5)$ [Δ]	12	36	24	1	0	1	[48] 24^1
$Q_4 = C_4 \times C_4$	16	32	16	1	0	1	[384] 64^1

References

[1] M. Brandt, W. Dickinson, A. Ellsworth, J. Kenkel, H. Smith, Optimal packings of two to four equal circles on any flat torus, Discrete Math. 342 (2019) 111597, 18 pages.
[2] M. Fréchet, Ky Fan, Initiation to Combinatorial Topology, Prindle, Weber & Schmidt, Boston, 1967.
[3] A. Gagarin, W. Kocay, D. Neilsen, Embeddings of small graphs on the torus, Cubo Mat. Educ. 5 (2) (2003) 351–371.
[4] F. Hadlock, Finding a maximum cut of a planar graph in polynomial time, SIAM J. Comput. 4 (3) (1975) 221–225.
[5] D. Hilbert, S. Cohn-Vossen, Geometry and the Imagination, Chelsea Publishing, New York, 1952.
[6] L. Christine Kinsey, Topology of Surfaces, Springer-Verlag, 1993.
[7] W. Kocay, Groups & Graphs – software for graphs, digraphs, and their automorphism groups, Match 58 (2) (2007) 431–443.
[8] W. Kocay, D. Kreher, Graphs, Algorithms, and Optimization, second ed., Chapman & Hall/CRC Press, Boca Raton, 2016.
[9] K. Kuratowski, Sur le problème des courbes gauches en topologie, Fund. Math. 15 (1930) 271–283, (French).
[10] S.A. Lavrenchenko, Irreducible triangulations of the torus, J. Sov. Math. 51 (5) (1990) 2537–2543.
[11] Bruce P. Mull, Enumerating the orientable 2-cell imbeddings of complete bipartite graphs, J. Graph Theory 30 (1999) 77–90.
[12] Bruce P. Mull, Robert G. Rieper, Arthur T. White, Enumerating 2-cell imbeddings of connected graphs, Proc. Amer. Math. Soc. 103 (1) (2008) 321–330.
[13] John Stillwell, Classical Topology and Combinatorial Group Theory, Springer Verlag, New York, 1980.
[14] John Stillwell, Geometry of Surfaces, Springer Verlag, New York, 1992.
[15] William P. Thurston, in: Silvio Levy (Ed.), Three Dimensional Geometry and Topology, Vol. 1, Princeton University Press, 1997.
[16] A. White, L. Beineke, Topological graph theory, in: L. Beineke, R. Wilson (Eds.), Selected Topics in Graph Theory, Academic Press, 1978.